

## Calculation of the van der Waals Potential Energy for Polyethylene and Polytetrafluoroethylene as Two-Atom and Three-Atom Chains: Rotational Freedom in the Crystals

BY L. D'ILARIO

*Laboratori Ricerche di Base, SNAM PROGETTI S.p.A., 00015 Monterotondo, Roma, Italy*

AND E. GIGLIO\*

*Laboratorio di Chimica Fisica, Istituto Chimico, Università di Roma, Italy*

(Received 28 September 1973; accepted 29 September 1973)

The van der Waals potential energy of polyethylene and polytetrafluoroethylene has been computed as a function of both two and three angles of rotation around the bonds of the backbone chain, the bond lengths and valence angles being held fixed. The calculations show that there are more minima than is predicted by the 'equivalence principle'. The implications of these results are important in the crystalline polymers and in the physical chemistry of the polymer solutions as well as in statistical-mechanical theories. In addition the evaluation of the van der Waals potential energy in the crystal of polytetrafluoroethylene by rotating in phase the polymer chains around their helical axes suggests that, surprisingly, the macromolecules are free-rotating.

### Introduction

It is well known that the conformations of polymers in crystals are governed almost completely by intramolecular interactions. The deepest minima of the potential energy of an isolated macromolecule correspond to the most stable conformations, one of which, generally, is found in the crystal (Liquori, 1961; De Santis, Giglio, Liquori & Ripamonti, 1963). Thus it is clear that the calculation of the potential energy for a polymer single chain provides a useful tool for solving the phase problem in the crystals.

The conformations of stereoregular macromolecules have been satisfactorily derived by means of the 'equivalence principle', assuming that such macromolecules are formed by identical monomeric units and that the torsion angles of one monomeric unit recur along the chain.

However, assumption of equivalence of the monomeric units in a polymer is justified only if the interactions among first neighbour monomeric units are by far the most important in stabilizing the macromolecule. Of course, the size and the geometry of the substituent atoms or groups linked to the skeleton atoms may cause the breakdown of the equivalence principle. This occurs if the second and higher neighbour interactions become competitive with the first neighbour ones.

In this paper we discuss the results of the van der Waals energy calculations performed for polyethylene (PET) and polytetrafluoroethylene (PFE) as a function of both two and three internal rotation angles.

Moreover the most stable conformations of PET and

PFE have been used in the qualitative estimate of the van der Waals energy in the crystals in order to investigate an unusual feature of PFE, namely the first-order crystalline transition which occurs at about 19°C.

### Conformational analysis of PET and PFE

If the equivalence principle is valid, the intramolecular potential-energy of PET and PFE depends on one internal angle of rotation and, therefore, these polymers are classified as one-atom chains (Hughes & Lauer, 1959). In what follows an internal rotation angle of 0° corresponds to the *cis* conformation. The lowest minima of PET and PFE have been found by several authors, using different sets of semi-empirical potentials, to be about 180° and 165° respectively (Birshtein & Ptitsyn, 1966, and references cited therein) together with those related by symmetry. Two other minima at about 60° and 90° are present in both the polymers.

The coefficients of the semi-empirical potentials employed by us in the generalized form:

$$V(r) = a \exp(-br)/r^d - cr^{-6}$$

are reported in Table 1. The potentials involving hydrogen and carbon atoms are those of Bartell (1960) previously verified in known and unknown crystal structures (Coiro, Giglio & Quagliata, 1972, and references quoted therein), while the F-F interactions have been described by a Ne-Ne potential proposed by Mason & Rice (1954). The electrostatic energy has been neglected because of the small difference between the electronegativities of the carbon and hydrogen atoms and because the minimum position of PFE is insensitive to the dipole-dipole interactions as shown by Iwasaki (1963),

\* To whom correspondence should be addressed.

Table 1. *Coefficients of the potentials used to describe the van der Waals interactions in PET and PFE*

The energy is in kcal/atom pair if  $r$  is in Å.

Interaction	$a \times 10^{-3}$	$b$	$c$	$d$
H-H	6.6	4.080	49.2	0
H-C	44.8	2.040	125.0	6
C-C	301.2	0.000	327.2	12
C-F	188.6	2.304	202.3	6
F-F	105.7	4.608	125.1	0

The values of the bond distances and bond angles used to calculate the van der Waals energy for a single chain and in the crystals are: PET: C-C=1.53 Å;

C-H=1.08 Å; C-C-C=112°; H-C-C=109.5°; PFE: C-C=1.54 Å; C-F=1.36 Å; C-C-C=114.6°; F-C-C=108.4°. The PFE geometry was derived by Iwasaki (1963) from the experimental X-ray data of Bunn & Howells (1954).

We have computed the van der Waals energy as a function of two and three torsion angles, supposing that the conformations of PET and PFE could be described by sequential pairs and triplets of angles  $(\psi_1, \psi_2)_n$  and  $(\psi_1, \psi_2, \psi_3)_n$ . The conformational analysis was performed varying the torsion angles by increments of 10° and the minima were subsequently explored by decreasing the angular increments to 5°. All interactions in a monomeric unit  $(CX_2)_2$  (X=H or F) and between this monomeric unit and the four nearest-neighbours which follow it have been calculated for a two-atom chain. The energy maps, reported in Figs. 1 and 2, show the mirror planes at  $\psi_1 = \psi_2$  and  $\psi_1 = 2\pi - \psi_2$  since the substituent atoms are all equal. The angular parameters defining some non-equivalent minima are given in Table 2. Although the energy values are merely qualitative and depend strongly on the potentials used, they are listed in order to allow a rough comparison among them. Table 3 contains similar results for the three-atom chains of PET and PFE, for which the energy has been evaluated by considering a monomeric unit  $(CX_2)_3$  and the two nearest-neighbours which follow it. Some significant sections of the three-dimensional energy map are shown in Figs. 3-6.

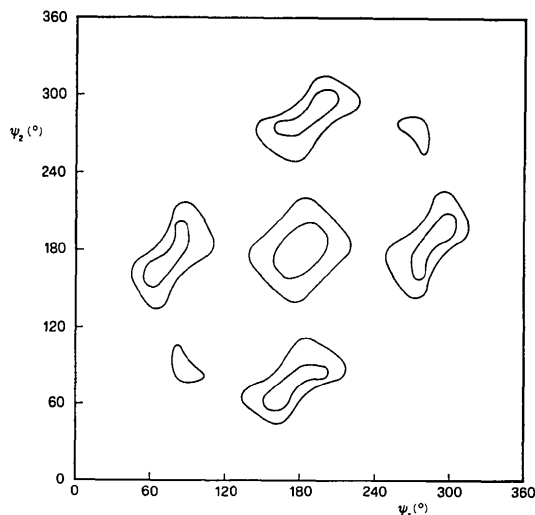


Fig. 1. Conformational van der Waals energy of PET as two-atom chain. The contour lines are drawn at 0.5 and 1.0 kcal.

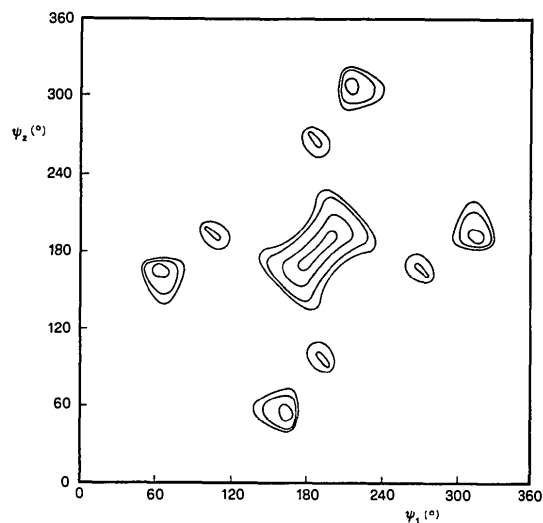


Fig. 2. Conformational van der Waals energy of PFE as two-atom chain. The contour lines are drawn at 0.5, 1.0, 2.0 and 2.5 kcal.

Table 2. *Van der Waals energy values of some PET and PFE minima as found in the two-atom chain conformational analysis*

	$\psi_1^{(0)}$	$\psi_2^{(0)}$	$V$ (kcal)
PET	180	180	0.2
	65	165	0.3
	85	190	0.4
	85	85	0.8
PFE	170	170	0.7
	55	165	1.3
	95	195	2.1

Table 3. *Van der Waals energy values of some PET and PFE minima as found in the three-atom chain conformational analysis*

	$\psi_1^{(0)}$	$\psi_2^{(0)}$	$\psi_3^{(0)}$	$V$ (kcal)
PET	180	180	180	0.4
	65	165	170	0.6
	60	60	160	0.6
	85	85	195	0.7
	85	85	90	1.3
	55	60	60	2.4
PFE	170	170	170	0.7
	55	165	165	1.2
	95	195	195	2.3
	60	60	155	3.4
	90	90	90	4.6

The same calculations were repeated with a very different set of potentials (Scott & Scheraga, 1966*b*). The minimum regions are unaltered, though the sequence of the lowest energy values is sometimes changed.

The two-atom chain energy map of PET presents the following outstanding features:

(i) a large flat minimum zone centred at  $\psi_1 = \psi_2 = 180^\circ$ . As an example the helix with  $\psi_1 = \psi_2 = 170^\circ$  differs from the zigzag planar chain by less than 0.1 kcal;

(ii) an elongated minimum region around  $\psi_1 = 65^\circ$  and  $\psi_2 = 165^\circ$ . The chain corresponding to this conformation has nearly the same energy as the *trans* one;

(iii) a third minimum at  $\psi_1 = \psi_2 = 85^\circ$  and a fourth one, not visible in Fig. 1, at about  $\psi_1 = \psi_2 = 60^\circ$  (*gauche* conformations) with much higher energy values;

(iv) the four deepest minima correspond to uniform and non-uniform helices which can be converted one into the other by overcoming rather low energy barriers (at most 1 kcal from our set of potentials).

The corresponding energy map of PFE shows:

(i) sharper minimum zones than those of PET;

(ii) the deepest minimum at  $\psi_1 = \psi_2 = 170^\circ$ ;

(iii) the second lowest minimum at  $\psi_1 = 55^\circ$  and  $\psi_2 = 165^\circ$  and the third at  $\psi_1 = 95^\circ$  and  $\psi_2 = 195^\circ$ . They lie approximately in the minimum region described in (ii) for PET;

(iv) a minimum of  $\sim 3$  kcal (not visible in Fig. 2) at about  $\psi_1 = \psi_2 = 90^\circ$  separated by a large barrier from a much higher minimum ( $\sim 11$  kcal) at about  $\psi_1 = \psi_2 = 60^\circ$ .

On the basis of these results it is clear that the energy maps of PET and PFE are very similar to those of polyisobutylene and polyvinylidene chloride (De Santis, Giglio, Liquori & Ripamonti, 1963) if treated as two-atom chains. Thus it is possible to locate the five deepest minima zones for the polymers with two equal groups bonded to each skeleton atom and described as a function of two torsion angles at about: (1)  $\psi_1 = \psi_2 = 180^\circ$ ; (2)  $\psi_1 = 60^\circ$ ,  $\psi_2 = 160^\circ$ ; (3)  $\psi_1 = 90^\circ$ ,  $\psi_2 = 200^\circ$ ; (4)  $\psi_1 = \psi_2 = 85^\circ$ ; (5)  $\psi_1 = \psi_2 = 60^\circ$ ; disregarding the symmetric minima. Of course the van der Waals radius of the substituents plays an important role in determining the position and the energy order of the minima. A gradual shift toward smaller values of  $\psi_1$  and  $\psi_2$  and higher values of the energy occurs for (1) if the steric hindrance of the atoms or groups increases. Since the substituents linked to the alternate carbon atoms of the skeleton chain give rise to interatomic distances of 2.5–2.6 Å the carbon chain tends to twist around the C–C bonds from the planar zigzag structure when the sum of the van der Waals radii of the substituents exceeds 2.6 Å. This always occurs for all substituents except hydrogen atoms. Analogous reasoning can be applied to explain the greater difference of the energies corresponding to the *gauche* conformations (4) and (5), taking into account that the interactions responsible

for this behaviour are mainly those among atoms attached both to adjacent carbon atoms of the skeleton and to carbon atoms separated by three bonds. Moreover the flat and elongated minimum (ii) of PET splits into two minima centred approximately at (2) and (3), the difference between the energies of (2) and (3) being more marked if the size of the substituents increases. Thus the minima (2) and (4) become deeper than (3) and (5) respectively.

It should be stressed that the occurrence of minima at (2) and (3) is peculiar for the one-atom chain and is not due to the different substituents of the two-atom chain.

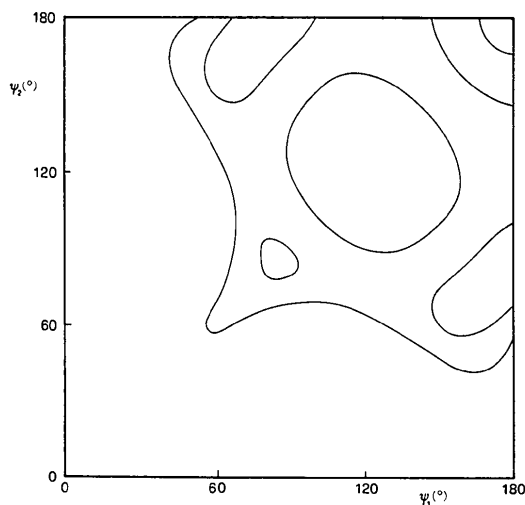


Fig. 3. Section at  $\psi_3 = 180^\circ$  of the van der Waals energy of PET. The contour lines are drawn at 0.5, 1.0 and 2.0 kcal.

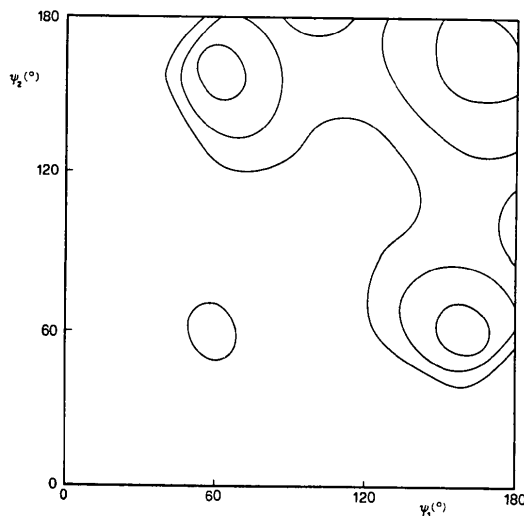


Fig. 4. Section at  $\psi_3 = 60^\circ$  of the van der Waals energy of PET. The contour lines are drawn at 1.0, 2.0 and 3.0 kcal.

The main features of the three-atom chain energy maps of PET and PFE can easily be summarized from the preceding results. By indicating with  $T$ ,  $G_1$  and  $G_2$  the rotational states of a C-C bond corresponding to a torsion angle of 180, 60 and 90° and excluding the enantiomorphous angles of 300 and 270°, the more probable conformations of PET and PFE can be written as:  $TTT$ ,  $G_1TT$ ,  $G_1G_1T$ ,  $G_2G_2T$ ,  $G_2TT$ ,  $G_2G_2G_2$ ,  $G_1G_1G_1$ . These rotational states can be derived from those of PET and PFE, treated as two-atom chains [see (1)–(5)]:  $TT$ ,  $G_1T$ ,  $G_2T$ ,  $G_2G_2$ ,  $G_1G_1$ , by further adding  $T$ ,  $G_1$  or  $G_2$ . It must be noted that a repeated sequence  $G_1G_2$  is energetically not favoured and that a polymer in  $G_1$  conformation is destabilized by short contacts between substituents linked to carbon atoms separated by three

bonds. Thus a quadruplet  $G_1G_1G_1G_1$  in the middle of a chain is very unlikely. As a consequence the rotational states corresponding to the minima of an  $n$ -atom chain with  $n > 3$  can be built up from the results obtained from the two and three-atom chain, bearing in mind the forbidden sequences.

The deepest minimum of both PET and PFE has been found in real crystals. Different conformations with greater spiral radius, corresponding to the other minima, cannot be advantageously realized in a crystal because they are associated with less dense packing and, obviously, with higher intermolecular energy. However these conformations can be compatible with the conditions characterizing the solution systems. Moreover it is reasonable to suppose the presence in the amorphous state of a mixture of chain segments having these conformations. It is also reasonable that the folded regions of PET may be at least partially formed by monomers in such conformations. This statement is supported by calculations of the potential-energy of folds and kinks in the PET crystal performed by Petraccione, Allegra & Corradini (1972) varying the torsion and the bond angles. Although the energy equation employed contains a van der Waals term, calculated by means of potentials (Abe, Jernigan & Flory, 1966) different from the ours, as well as two more terms due to C-C-C bending and to the hindering potential arising in the rotation around C-C bonds, the minima found by them for short kinks and folds in the 200 and 110 planes of the orthorhombic crystal structure of polyethylene can be written as:

Plane 200 fold:  $TTTTG_1TG_1G_1TTT$  ( $G_1^* = 300^\circ$ )

Plane 110 fold:  $TTG_1TG_1G_2G_1^*G_1^*TTT$

Reneker kink (Reneker, 1962):  $TTTTG_1G_2G_1TTTT$  and are in agreement with some minima which can be deduced from our results applied to short chains.

These results, in connection with those of Scott & Scheraga (1966a) on the rotational states of normal hydrocarbons, reinforce the hypothesis that a very high number of rotational conformers are needed to describe a polymeric system by means of statistical-mechanical theories. Therefore the procedure adopted until now of taking into account only a few rotational states is an oversimplification.

#### Potential-energy calculations in PET and PFE crystals

PFE is a highly crystalline, chemically inert and thermally stable polymer. However PFE shows unusual crystal transitions at about 19 and 30°C, temperatures very far from the 'melting point', about 330°C, which represents the first order transition from a partly crystalline to an amorphous structure. The crystal transitions at room temperatures were investigated by Bunn & Howells (1954) and Clark & Muus (1962a,b) by X-ray diffraction. Below 19°C PFE crystallizes in a triclinic or monoclinic phase, relatively ordered and nearly hexagonal with the parameters (0°C):

$$a = b = 5.59; c = 16.88 \text{ \AA}; \gamma = 119.3^\circ.$$

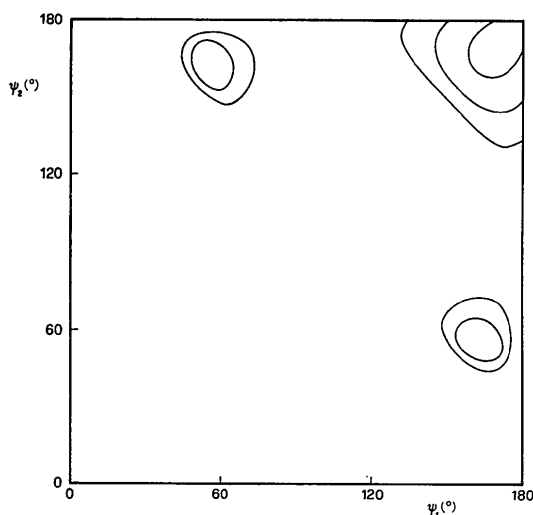


Fig. 5. Section at  $\psi_3 = 170^\circ$  of the van der Waals energy of PFE. The contour lines are drawn at 1.0, 2.0 and 3.0 kcal.

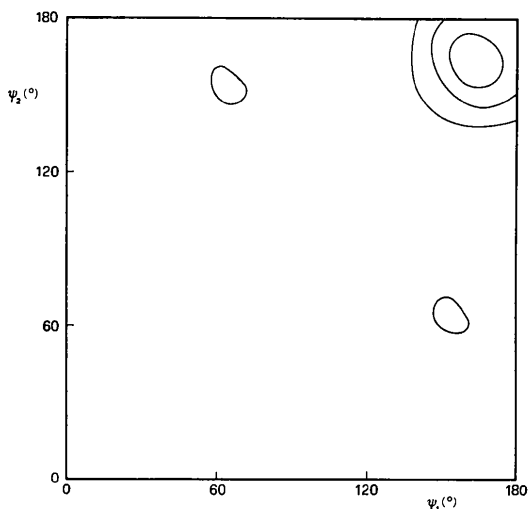


Fig. 6. Section at  $\psi_3 = 60^\circ$  of the van der Waals energy of PFE. The contour lines are drawn at 2.0, 3.0 and 5.0 kcal.

Above 19°C the unit cell is supposed to be trigonal, the chains being partially disordered and packed into a hexagonal lattice with dimensions (25°C):

$$a = 5.66; c = 19.50 \text{ \AA}.$$

At the 19°C transition the helical macromolecule changes its repeat unit from 13 CF<sub>2</sub> groups arranged in 6 turns to 15 CF<sub>2</sub> groups in 7 turns. If the geometry of Iwasaki (1963) is assumed, the one-atom chain of PFE is characterized by internal rotation angles of 163.5 and 165.7° for the 13<sub>6</sub> and 15<sub>7</sub> helices respectively, in good agreement with the potential-energy calculations.

It is believed (Clark & Muus, 1962*b*) that the disorder arises from torsional oscillations coupled with a gradual untwisting of the helical polymer. In order to assess qualitatively the barriers hindering the rotation of the macromolecules around their helical axes as well as the role of the conformation, we have performed calculations of van der Waals energy in triclinic and hexagonal crystal phases with the unit-cell constants previously quoted. The helical axes have been supposed to be perpendicular to the *ab* plane. Chains of fourteen and sixteen CF<sub>2</sub> groups in 13<sub>6</sub> and 15<sub>7</sub> conformations were rotated counterclockwise in the triclinic and hexagonal cells by the same angle  $\varphi$ .  $\varphi = 0^\circ$  corresponds to a helix with the first carbon atom lying on the *X* axis of an orthogonal framework *OXYZ* having *Y* and *Z* coinciding with the *b* and *c* crystallographic axes and *X* in the *ab* plane. The van der Waals energy was computed with the potentials of Table 1, considering all the interactions between one central chain and those adjacent to it. Very astonishingly the energy does not vary as a function of  $\varphi$  for either crystal (see the thin line of Fig. 7 for the 13<sub>6</sub> helix). A property of the 13<sub>6</sub> and 15<sub>7</sub> conformations is a rather uniform distribution of the fluorine atoms, which control the packing, over the cylindrical surface of their helices. Moreover space-filling models of the 13<sub>6</sub> and 15<sub>7</sub> helices do not show any pronounced protrusion. These peculiar features and the mutual arrangement of the chains give rise to molecular contacts between fluorine atoms, ranging approximately from 2.65 to 2.85 Å, and continuously reforming during the rotation.

The same calculation was performed for *trans*-planar helices in order to investigate the influence of the conformation. The change from 163.5 to 180° in the internal rotation angle determines the occurrence of energy barriers (see the thick line of Fig. 7) because a fully extended conformation shows all the substituents gathered in two parallel planes perpendicular to the plane of the backbone. Thus the fluorine atoms, protruding on two opposite sides, do not allow a suitable hexagonal or pseudo-hexagonal packing, which is favoured by the uniform arrangement of the substituents on a cylindrical surface. This in part may explain, for example, why the *trans*-planar chains of PET do not crystallize in the hexagonal system. On the other hand there is a lack of prominent barriers if the torsion angle is in the range 130–170°.

For comparison we have performed similar calculations for the orthorhombic unit cell of PET, space group *Pnam* (Bunn, 1939), with dimensions:

$$a = 7.41; b = 4.94; c = 2.55 \text{ \AA},$$

taking into account the crystal symmetry. All interactions between a central (CH<sub>2</sub>)<sub>2</sub> unit and the eight nearest (CH<sub>2</sub>)<sub>4</sub> chain segments were considered. The van der Waals energy as a function of  $\varphi$  is reported in Fig. 8. The potentials of Table 1 were used and the actual structure differs from the minimum at 43° by 6°. The PET energy barriers are much higher than those

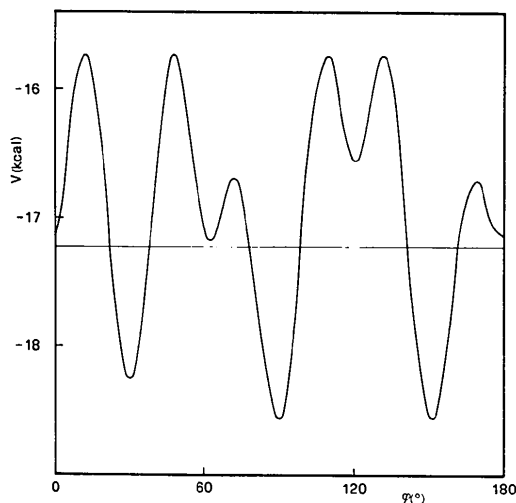


Fig. 7. Van der Waals energy  $V$  of PFE chains in the triclinic unit cell as a function of the rotation angle around the helical axes. The thin and thick lines refer to the 13<sub>6</sub> and *trans* planar conformations respectively.

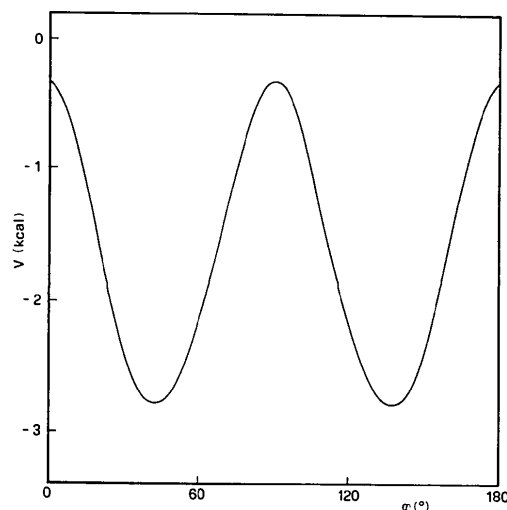


Fig. 8. Van der Waals energy  $V$  of PET in the orthorhombic unit cell vs. the rotation angle  $\varphi$  around the helical axes.  $\varphi = 0^\circ$  corresponds to carbon atoms of the central chain with *y* coordinate equal to 0.

of PFE in the zigzag planar conformation (see Fig. 7) although the F-F are stronger than the H-H interactions. Transitions from orthorhombic or monoclinic phases to the hexagonal one are well-known in many n-paraffin crystals. Such transformations involve the rotational degree of freedom of the hydrocarbon mole-

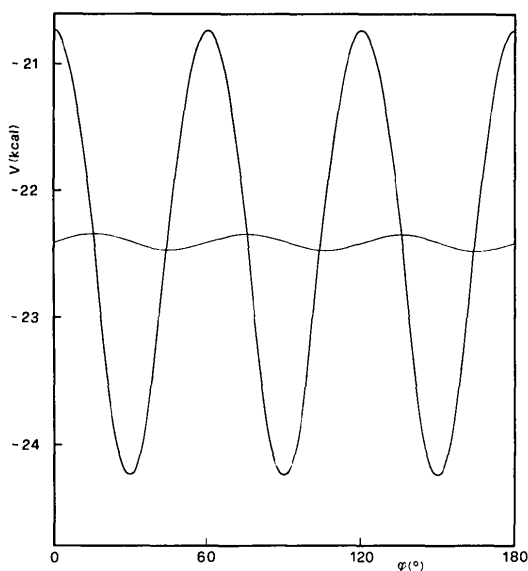


Fig. 9. Van der Waals energy  $V$  of chains containing 16  $\text{CH}_2$  groups in a hexagonal cell vs. the rotation angle  $\phi$  around the helical axes. The flattened curve refers to a torsion angle of  $165^\circ$ , the other one to  $180^\circ$ .

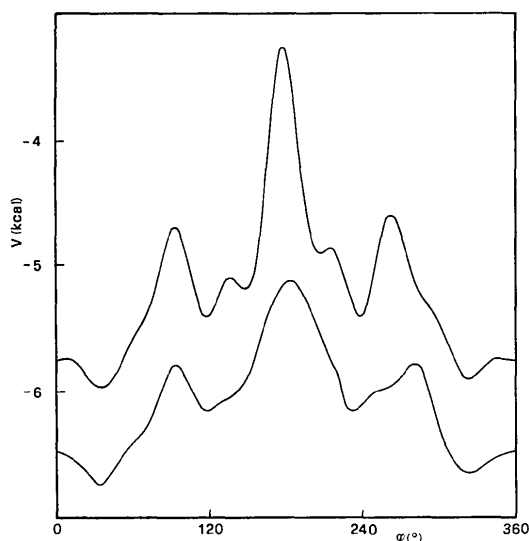


Fig. 10. Van der Waals energy between two chains of PFE as a function of the rotation angle  $\phi$  around the helical axis of one chain, the other being held fixed. Upper curve:  $13_6$  helix, fourteen  $\text{CF}_2$  in every chain; lower curve:  $15_7$  helix, sixteen  $\text{CF}_2$  in every chain.

cules and occur near the melting point. It is plausible that the hexagonal packing can be favoured by a change of conformation, passing from an internal rotation angle of  $180^\circ$  to a slightly lower value as in PFE. In this connexion the large flat zone of the global minimum of PET must be remembered (see (i) of the two-atom chain of PET and Fig. 1), for which small adjustments in the torsion angles are permissible.

It is also interesting to rotate n-paraffin helices in a hexagonal cell with the same rules as for the  $15_7$  spiral of PFE. The  $a$  and  $b$  axes were taken equal to  $4.77 \text{ \AA}$  as found in the hexagonal form of n-tetracosane,  $\text{C}_{24}\text{H}_{50}$ , stable at  $46.5^\circ\text{C}$  (Mazee, 1948). The results are like those of PFE (see Fig. 9) so that the onset of rotation around the chain axes in paraffin crystals may be more easily explained with a slightly distorted *trans* planar conformation. As an example a  $(\text{CH}_2)_n$  chain with  $\text{C}-\text{C}-\text{C} = 112^\circ$  and  $15_7$  helical symmetry has a  $3_1$  screw axis if the internal rotation angle is  $165.5^\circ$ .

In addition we have investigated what happens if one  $13_6$  or  $15_7$  chain of PFE is held fixed and another of the same kind is rotated around the helical axis at a distance of  $5.59$  or  $5.66 \text{ \AA}$ . The values of the van der Waals energy vs.  $\phi$  are plotted in Fig. 10. As expected the energy barriers decrease for the  $15_7$  helix, to which can be assigned in the hexagonal phase a rotational freedom greater than that of the  $13_6$  helix in the triclinic cell. This is in agreement with both the appearance of diffuse streaks in the X-ray fibre pattern (Clark & Muus, 1962b) and the nuclear magnetic resonance results (Hyndman & Origlio, 1960; McCall, Douglass & Falcone, 1967) at temperatures between  $19$  and  $30^\circ\text{C}$ .

However the disorder may also arise from the inversion of the PFE helices, which can exist in two equivalent conformations with torsion angles of about  $165$  and  $195^\circ$ , as well as from torsional oscillations along the chains. As the temperature is increased toward  $19^\circ\text{C}$  these effects are enhanced, but it seems probable that at least rotations of the macromolecules around their helical axes below  $19^\circ\text{C}$  occur in the oblique unit cell.

## References

- ABE, A., JERNIGAN, R. L. & FLORY, P. J. (1966). *J. Amer. Chem. Soc.* **88**, 631-639.
- BARTELL, L. S. (1960). *J. Chem. Phys.* **32**, 827-831.
- BIRSHTEN, T. M. & PTITSYN, O. B. (1966). *Conformations of Macromolecules*, pp. 72-84. New York: Interscience.
- BUNN, C. W. (1939). *Trans. Faraday Soc.* **35**, 482-491.
- BUNN, C. W. & HOWELLS, E. R. (1954). *Nature, Lond.* **174**, 549-551.
- CLARK, E. S. & MUUS, L. T. (1962a). *Z. Kristallogr.* **117**, 108-118.
- CLARK, E. S. & MUUS, L. T. (1962b). *Z. Kristallogr.* **117**, 119-127.
- COIRO, V. M., GIGLIO, E. & QUAGLIATA, C. (1972). *Acta Cryst.* **B28**, 3601-3605.
- DE SANTIS, P., GIGLIO, E., LIQUORI, A. M. & RIPAMONTI, A. (1963). *J. Polymer Sci.* **A1**, 1383-1404.

- HUGHES, R. E. & LAUER, J. L. (1959). *J. Chem. Phys.* **30**, 1165–1170.
- HYNDMAN, D. & ORIGLIO, G. F. (1960). *J. Appl. Phys.* **31**, 1849–1852.
- IWASAKI, M. (1963). *J. Polymer Sci. A1*, 1099–1104.
- LIQUORI, A. M. (1961). *Chimica Inorganica, IV Corso Estivo di Chimica, Varenna*, 1959, pp. 311–333. Ed. Accad. Nazl. Lincei, Roma.
- MCCALL, D. W., DOUGLASS, D. C. & FALCONE, D. R. (1967). *J. Phys. Chem.* **71**, 998–1004.
- MASON, E. A. & RICE, W. E. (1954). *J. Chem. Phys.* **22**, 843–851.
- MAZEE, W. M. (1948). *Rec. Trav. Chim. Pays-Bas*, **67**, 197–213.
- PETRACCONE, V., ALLEGRA, G. & CORRADINI, P. (1972). *J. Polymer Sci. C38*, 419–427.
- RENEKER, D. H. (1962). *J. Polymer Sci.* **59**, S39–42.
- SCOTT, R. A. & SCHERAGA, H. A. (1966a). *J. Chem. Phys.* **44**, 3054–3069.
- SCOTT, R. A. & SCHERAGA, H. A. (1966b). *J. Chem. Phys.* **45**, 2092–2101.

*Acta Cryst.* (1974). **B30**, 378

## The Crystal and Molecular Structure of a Monoclinic Phase of Iminodiacetic Acid

BY C.-E. BOMAN, H. HERBERTSSON AND Å. OSKARSSON

*Inorganic Chemistry 1, Chemical Center, University of Lund, P.O.B. 740, S-220 07 Lund, Sweden*

(Received 12 October 1973; accepted 16 October 1973)

The crystal and molecular structure of a monoclinic phase of iminodiacetic acid,  $C_4H_7NO_4$ , has been determined from X-ray intensity data obtained with a four-circle diffractometer. The space group is  $P2_1/c$  with  $Z=4$ ,  $a=6.3406$  (7),  $b=9.1364$  (6),  $c=9.3783$  (13) Å and  $\beta=92.72$  (1)°. The structure ( $R=0.040$ ) is a three-dimensional network of 10- and 14-membered rings composed of hydrogen-bonded halves of the iminodiacetic acid molecule. There are three independent hydrogen bonds in the structure. Two of them are of the type  $N-H\cdots O$  with lengths 2.674 (2) and 2.807 (2) Å, and one is of the type  $O-H\cdots O$  with the length 2.536 (2) Å.

### Introduction

The structures of a number of compounds containing the iminodiacetic acid group have been reported. In these structures the iminodiacetic acid residue acts as a monodentate or a tridentate ligand coordinated to lanthanoid(III) ions (Albertsson & Oskarsson, 1968; Oskarsson, 1971) or as a donor of hydrogen bonds to halide ions (Oskarsson, 1973). The organic molecule shows a large conformational variation in these compounds. In order to study the effect of different crystallographic surroundings upon the geometry of the iminodiacetic acid group we have determined the structure of the acid. A comparison with oxydiacetic acid (Herbertsson & Boman, 1973) and thiodiacetic acid (Paul, 1967) should also give some information concerning the effect of the atom (O, S or N) between the acetic acid residues upon packing and hydrogen bonding.

Three different modifications of iminodiacetic acid, denoted  $\alpha$ ,  $\beta$  and  $\gamma$ , have been reported by Tomita, Ando & Ueno (1964). Novak, Cotrait & Jousot-Dubien (1965) have studied the infrared spectrum of iminodiacetic acid in the solid state ( $\alpha$ -phase) and they conclude that it is a zwitterion. In this communication the crystal and molecular structure of a monoclinic phase corresponding to the  $\beta$ -phase is reported and is referred to below as IMDAMO.

### Crystal data

Iminodiacetic acid,  $C_4H_7NO_4$  (IMDAMO); F. W. 133.1; Monoclinic, space group  $P2_1/c$ ;  $a=6.3406$  (7),  $b=9.1364$  (6),  $c=9.3783$  (13) Å,  $\beta=92.72$  (1)°,  $V=542.7$  Å<sup>3</sup>;  $Z=4$ ;  $\mu(Cu K\alpha)=13.0$  cm<sup>-1</sup>;  $D_m=1.64$ ,  $D_x=1.629$  g cm<sup>-3</sup>. Numbers within parentheses represent estimated standard deviations.

### Experimental

Commercial iminodiacetic acid (BDH, Chemicals Ltd., Poole, England) was recrystallized from water by slow evaporation at room temperature. Two colourless solid phases were obtained, one needle-shaped and the other short prismatic. For both phases elemental analyses gave values in good agreement with those calculated for  $C_4H_7NO_4$ . The density  $D_m$  was determined from the loss of weight in benzene. Weissenberg photographs showed the needle-shaped crystals to be orthorhombic and the short prismatic ones to be monoclinic. The systematically absent reflexions for IMDAMO are  $0k0$  with  $k \neq 2n$  and  $h0l$  with  $l \neq 2n$ , which are consistent with the space group  $P2_1/c$ . The unit-cell dimensions were improved by a least-squares treatment of powder spectra obtained with a Guinier-Hägg focusing camera (Cu  $K\alpha_1$  radiation,  $\lambda=1.54051$  Å, 22°C). Alu-